Elastic Properties of Grinding Wheel

By

Kenjiro OKAMURA* and Toshikatsu NAKAJIMA*

(Received June 27, 1969)

The properties of grinding wheel have been presented by the "grade" measured by the scale of plastic deformation. However in order to clarify the behavior of a cutting edge during grinding, the properties of grinding wheel should be indicated by the value measured by the scale of elastic deformation.

From the above mentioned point of view, in this paper the three-dimensional distribution of cutting edges which are necessary for analyzing the spring constant is first made clear and then the spring constant of grain mounting is analyzed to discuss the relation between the spring constant and grain size, bond material, bond ratio and dressing conditions.

1. Introduction

The properties of grinding wheels have been presented by the "grade" that indicates the bonding forces between grains and the cleavage force of abrasive grains. Many methods for measuring the grade have been proposed by numerous researchers[1),2)]. The grade can be seen to be an important value from the point of view of the wear of the grinding wheel, but it does not immediately indicate the behavior of the cutting edges during grinding.

In order to clarify the behavior of the cutting edge during grinding, it would be better if the properties of the grinding wheel could be represented by the amount of elastic deformation.

The effect of the elastic properties of grinding wheels on the grinding process has been pointed out by R.S. Hahn[3)] and the authors. Dr. R.S. Hahn discussed the effect of elastic displacement of cutting edges on the grinding process for the first time; and we have pointed out that the sliding length of the cutting edge at the beginning of a cut is a function of the spring constant of the grain mounting and that the spring constant has, therefore, a close relation to the grinding results such as surface roughness and depth of the work-hardened layer.

A mentioned above, the properties of the grinding wheel must be described by

* Department of Precision Mechanics

the amount of elastic displacement of the grain for the grinding process analyzed from the fundamental point of view.

There are two directions in studies on the elastic properties of the grinding wheel. One is the direction where the modulus of elasticity of the wheel composed of abrasive, bond and pore is measured[4),5)] and the other is the elastic displacement of each grain resiliently mounted by bond bridges[2)].

The former is useful for macroscopic deformation of the wheel and the control of vibrations of the grinding system. But in practial grinding and from the point of view of chip formation physics each grain in the interference zone bears the grinding load and displaces almost separately.

Therefore, the spring constant of grain mounting will be more useful to the grinding process in terms of basic chip formation, than the modulus of elasticity of the wheel.

In this paper the three-dimensional distribution of cutting edges which is necessary for analyzing the spring constant will be discussed and then the spring constant of grain mounting will be measured. The relation between the spring constant and grain size, bond materials, bond ratio and dressing conditions will also be shown.

2. Three-Dimensional Distribution of Cutting Edges

The three-dimensional distribution of cutting edges will be necessary for the spring constant to be measured. The distribution of cutting edges on the surface of the wheel has been measured in many different ways by numerous researchers. But all have been two-dimensional studies. In other words, the cutting edges are supposed to be distributed on the same surface of wheel. In actual wheels, the cutting edges aren't distributed on the same surface and, therefore, the distribution of cutting edges will be a function of the depth from the surface of the wheel. In this section the distribution of cutting edges will be measured three-dimensionally and the relation between the distribution and grain size, bond ratio and dressing conditions will be discussed.

2.1 Experimental Method

The profile of the surface of the wheel is measured with a Proficorder immediately after dressing the wheel. From the profile curve obtained the three-dimensional density of cutting edges can be calculated statistically. In order to check the correspondence of cutting edges with the profile curve, a microphotograph of the same part of the surface of wheel where the profile is measured will be taken and compared with the profile curve.

Further more the number of cutting edges will also be measured by the classical method, that is, the direct contact method and compared with the value calculated statistically. Figure 1 shows one of the classical direct contact methods. As easily

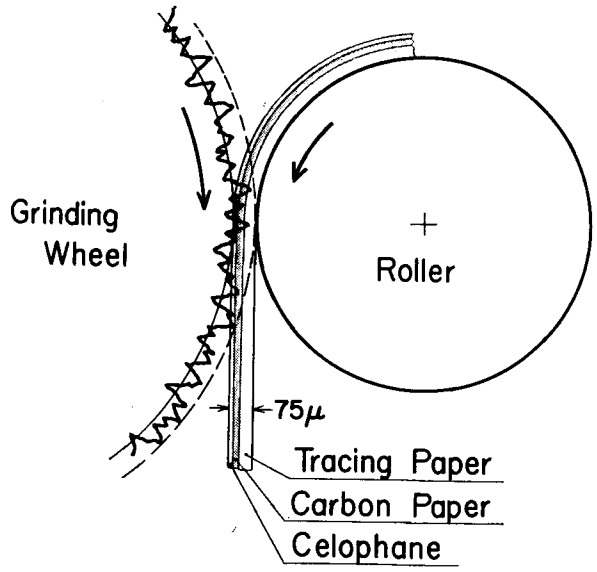

Fig. 1. Direct contact method of measuring cutting edges

seen in this figure the distance between wheel and work is set up to be zero and then the known thickness of paper composed of tracing and carbon paper is fed between the wheel and the workpiece.

Table 1.

Bond	Abrasive	Grade	V_G	V_B	V_P
Vitrified Bond	WA 36	K	m		
	WA 60	H	0.480	0.106	0.414
		L	0.480	0.177	0.343
		P	0.480	0.247	0.273
	WA 120	K	m		
Resinoid Bond	WA 60	H	0.470	0.125	0.405
		L	0.470	0.165	0.365
		P	0.470	0.215	0.315
P.V.A.	WA 60	$7M_2$			
		$13M_2$			
		$15M_2$			

Table 2. Dressing condition 1800 rpm.

	t_d (μ)	V_{fd} (mm/rev. of G.W.)
a	2.5	0.05
b	20	0.20
c	40	0.40

In this experiment the thickness of the paper is 75 μ and, therefore, all of the cutting edges that exist from the surface of the wheel to a depth of 75 μ are measured by this method.

Table 1 and Table 2 show the wheels and dressing conditions used throughout these experiments.

2.2 Calculating Method of Density of Cutting Edges.

There will be many methods to calculate the density of cutting edges from the profile curve. In this experiment two methods as follows are used:

(1) Direct Counting Method

This is a method by which the density of cutting edges can be counted directly from the profile curve. As shown in Figure 2(a), the profile curve is divided uniformly parallel to the base line from the surface of wheel and then the number of peaks (M_i) which occur at a depth corresponding to a function of the average grain size is the number of cutting edges. The total number of cutting edges from the surface down to the depth u is given by the value ΣM_i and is a function of the depth u from the surface. Then the average cutting edge spacing $w(u)$ will be given as a function of the depth u in the form

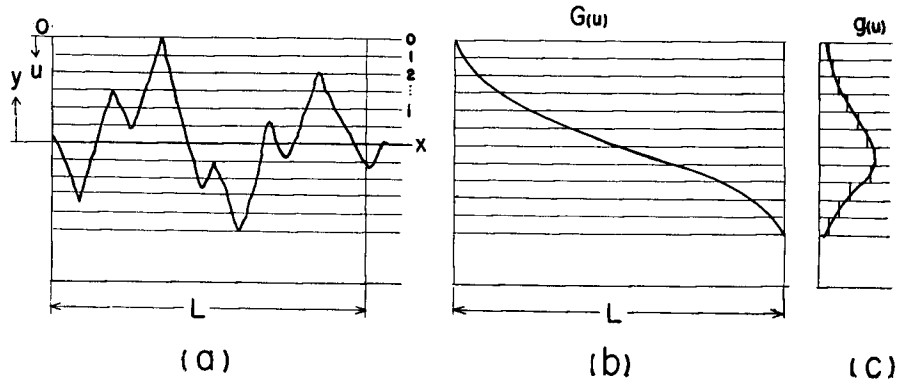

Fig. 2. Cutting edge distribution curve
(a) Profile of grinding wheel surface
(b) Cumulative distribution curve
(c) Cutting edge distribution curve

$$w(u) = \frac{L}{\Sigma M_i} \tag{1}$$

where L is the measuring length. On the assumption that the profile curve is statistically the same in any direction the average density of cutting edges $\lambda(u)$ will be as follows from Equation (1),

$$\lambda(u) = \left(\frac{\Sigma M_i}{L}\right)^2 \tag{2}$$

(2) Statistical Calculating Method

First the profile curve is divided uniformly parallel to the base line as shown in Figure 2(a). By measuring the total length of a part of the profile curve cut off by a parallel line we can get the cummulative distribution curve as shown in Figure 2(b). Then by measuring the difference of length between divisions and normalizing we can get the distribution curve $g(u)$ as shown in Figure 2(c). The Distribution curve $g(u)$ should be proportional to the increment of the cummulative distribution curve $G(u)$, then

$$\frac{dG(u)}{du} = L \cdot g(u) \tag{3}$$

For this study it is assumed that grains are perfect spheres and do not break as they are dressed. Now consider an imaginary section at a depth u from the surface of the wheel.

On this imaginary section, the cutting edges have a diameter between 0 and $\sqrt{(u+\delta)d_0-(u+\delta)^2}$ and are assumed to be distributed at random. Therefore, the average distribution diameter of the cutting edges $\bar{d}(u)$ is given by the equation

$$\bar{d}(u) = \sqrt{\frac{2}{3}[3d_0(u+\delta)-2(u+\delta)^2]} \tag{4}$$

where δ is the amount of grain diameter removed by dressing. Cutting edges of diameter $\bar{d}(u)$ will be distributed over the length given by the cumulative distribution curve $G(u)$ and then the average cutting edge spacing $w(u)$ is given in the form

$$w(u) = L \cdot \frac{\bar{d}(u)}{G(u)} \tag{5}$$

Supposing again that the profile curve is statistically the same in any direction, the density of cutting edges $\lambda(u)$ at the depth u from the surface of wheel is given by the equation

$$\lambda(u) = \frac{3}{2[3d_0(u+\delta)-2(u+\delta)^2]}\left\{\int_\delta^u g(u)du\right\}^2 \qquad (6)$$

2.3 Correspondence of the Peaks in the Profile Curve with Cutting Edges

As mentioned in the previous section, the number of cutting edges can be calculated statistically from the profile curve of the surface of wheel. Therefore, the correspondence of the peaks in the profile curve with cutting edges should be checked. Figure 3(a) shows some part of the grinding wheel dressed under the condition (c) and Figure 3(b) the results obtained by the classical direct contact method. In these figures the white parts correspond to cutting edges.

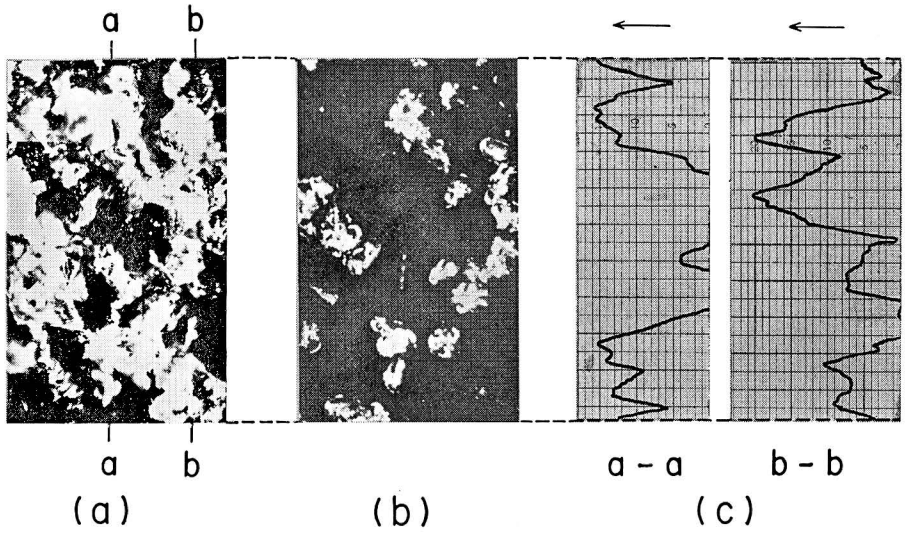

Fig. 3. Correspondence of peaks in the profile curve with cutting edges

The profiles on the lines a-a and b-b are shown in Figure 3(c) respectively. As seen in these figures, the peaks of the profile curve correspond very well to the cutting edges and, therefore, the density of the cutting edges can be statistically calculated from the profile curve.

2.4 Analytical Form of the Distribution Curve

The form of the distribution curve $g(u)$ must be known before the three-dimensional distribution of cutting edges can be calculated, but it takes a lot of time to calculate the statistics for the curve $g(u)$ for each case.

If we could find some characteristic values from which the analytical form of the distribution curve could be determined, we could easily calculate the

three-dimensional distribution of cutting edges by analyzing the relation between the characteristic values and grain size, bond ratio and dressing conditions.

From the above mentioned point of view, some characteristic values which determine the distribution curve $g(u)$ will be introduced by discussion of the curve $g(u)$ and the relation between these characteristic values and grain size, bond ratio and dressing conditions. The histograms in Figure 4 show the normalized distribution of cutting edges calculated from the profiles of the surface of the wheel dressed under three different conditions *a*, *b* and *c*.

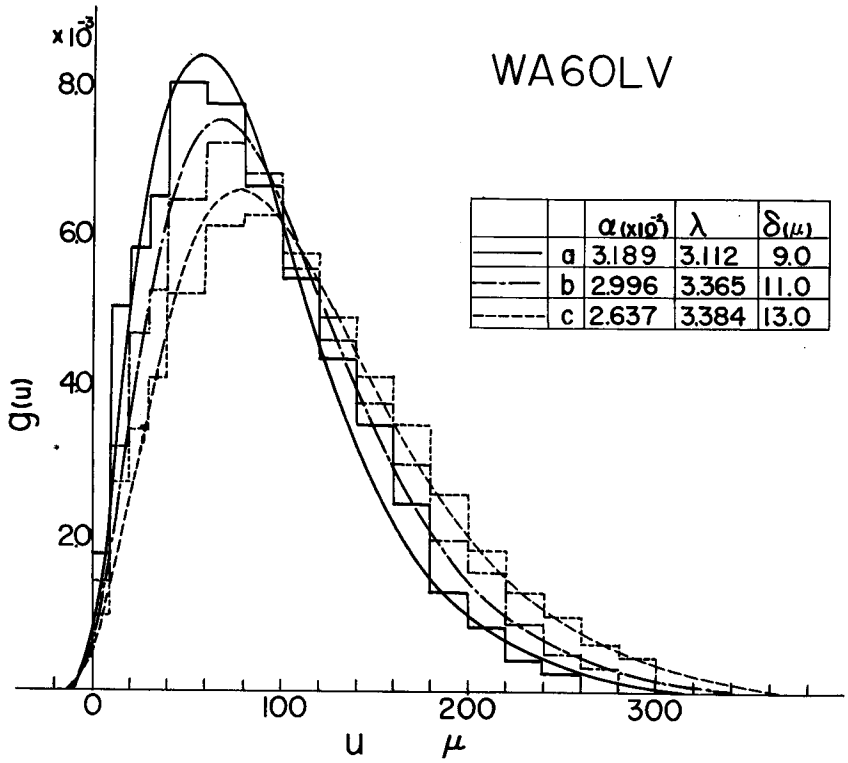

Fig. 4. Normalized cutting edge distribution

From this figure it can be seen that the value of the curve $g(u)$ increases rapidly near the surface of the wheel, becomes maximum at a certain point and then decreases. Therefore, the analytical form of the distribution curve $g(u)$ may be represented by the modified Γ-distribution function.
That is,

$$g(u) = \frac{\alpha^{\lambda}}{\Gamma(\lambda)}(u+\delta)^{\lambda-1}e^{-\alpha(u+\delta)} \qquad (7)$$

where δ is a value which should be calculated from the average initial area

assuming that the abrasive is a sphere and α and λ are characteristic values by which the Γ-distribution can be determined and are given by the mean value $\bar{x}$ and the variance s^2 of the $g(u)$ distribution as follows:

$$\alpha = \bar{x}/s^2, \quad \lambda = \bar{x}^2/s^2 \tag{8}$$

The curves in Figure 4 show the value calculated by Equation (7). From the comparison of the curves with the histogram it can be seen that we will be able to adopt the Γ-distribution function (7) for the analytical form of the distribution curve $g(u)$. In Equation (7) characteristic values α, λ and δ should be calculated statistically to get the analytical form of the distribution curve $g(u)$. Therefore, the relation between these characteristic values and grain size, bond ratio and dressing conditions will be discussed successively.

Figure 5 shows the variation of the characteristic values α and λ with the bond ratio for a vitrified bond wheel (abrasive Al_2O_3, grain size 60) and Figure 6 that for a resinoid bond wheel (abrasive Al_2O_3, grain size 60). Figure 7 also shows the variation of the values α and λ with the grain size for vitrified bond wheel (abrasive Al_2O_3). In these figures the dressing conditions are parameters. Figure 8 and Figure 9 show the variation of the value δ with the bond ratio for the vitrified and the resinoid bond wheel respectively. Figure 10 shows the variation of the value δ with grain size. In Figure 5 to Figure 10 we can find the relation between the characteristic values α, λ and δ and grain size, bond ratio and dressing conditions and, therefore, determine the analytical form of the distribution curve $g(u)$. Figure 11 shows an example of the analytical curve $g(u)$ for the distribution of cutting edges calculated by Equation (7) for the different sizes of grain.

2.5 Three Dimensional Density of Cutting Edges

In a practical grinding wheel the cutting edges are not on the same surface but are distributed three dimensionally. Therefore, the density of cutting edges should be measured three-dimensionally. There are two methods for evaluating the three-dimensional density of cutting edges from the profile curve of the surface of the wheel as mentioned above. One is the method by which the density is calculated directly and the other is that by which the three-dimensional density of cutting edges is calculated statistically from the distribution curve $g(u)$. In the latter method the analytical form of the distribution curve $g(u)$ can be represented in the Equation (7), so that the three-dimensional density $\lambda(u)$ of cutting edges can be evaluated as the function of the depth u from the surface of the wheel by the equation

$$\lambda(u) = \frac{3\alpha^{2\lambda}}{[6d_0(u+\delta)-4(u+\delta)^2]\Gamma(\lambda)^2}\left[\int_{\delta}^{u}(u+\delta)^{\lambda-1}e^{-\alpha(u+\delta)}du\right]^2 \tag{9}$$

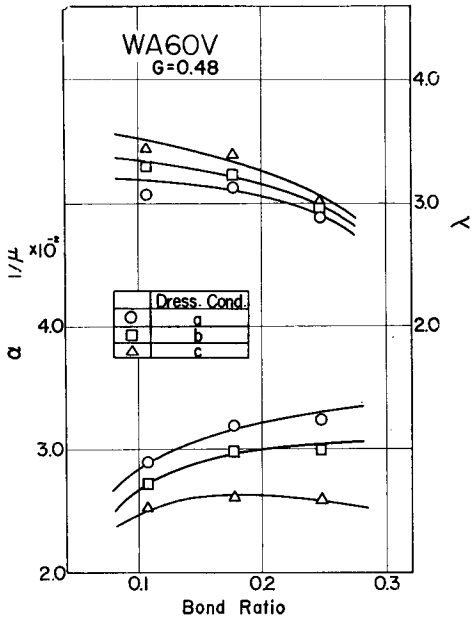

Fig. 5. Variations of α, λ distribution parameters with bond ratio (Vitrified Wheel)

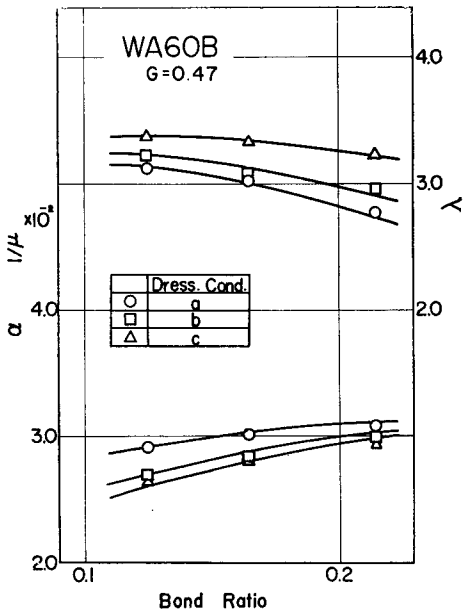

Fig. 6. Variations of α, λ distribution parameters with bond ratio (Resinoid Wheel)

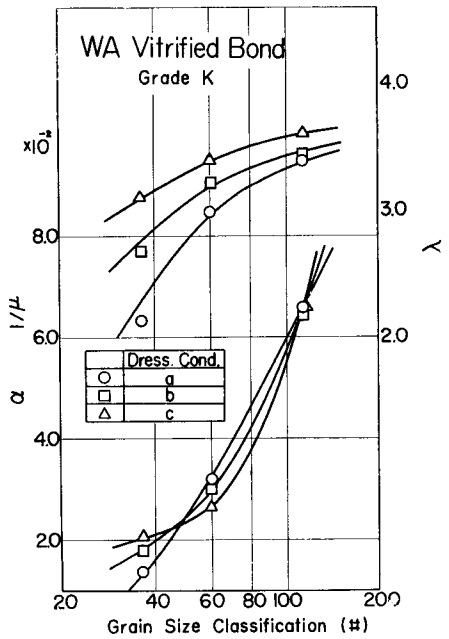

Fig. 7. Variations of α, λ distribution parameters with grain size (Vitrified Wheel)

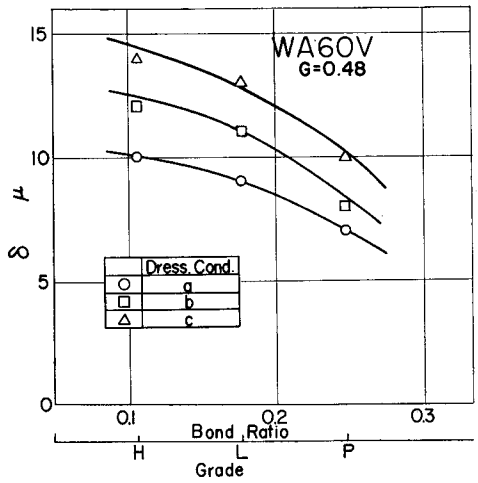

Fig. 8. Variations of α, λ distribution parameter with bond ratio (Vitrified Wheel)

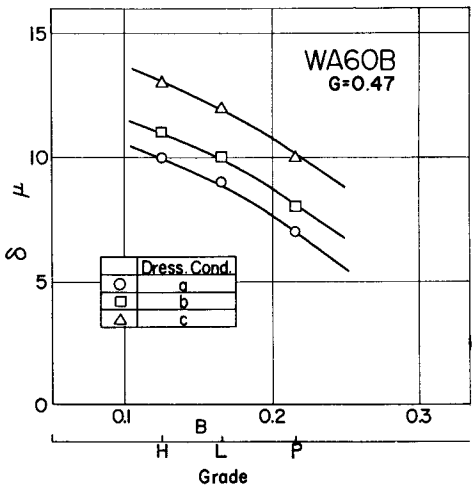

Fig. 9. Variations of δ distribution parameter with bond ratio (Resinoid wheel)

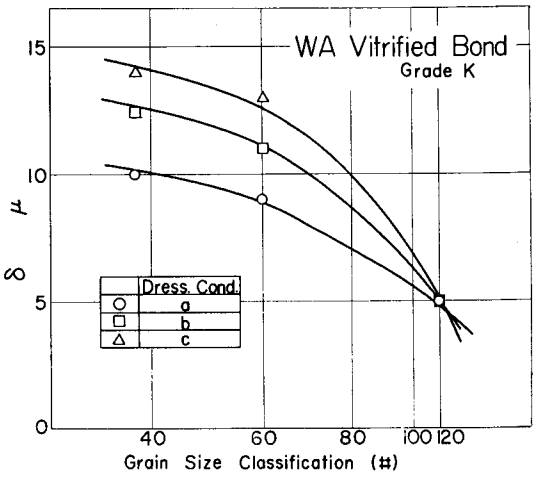

Fig. 10. Variations of δ distribution parameter with grain size

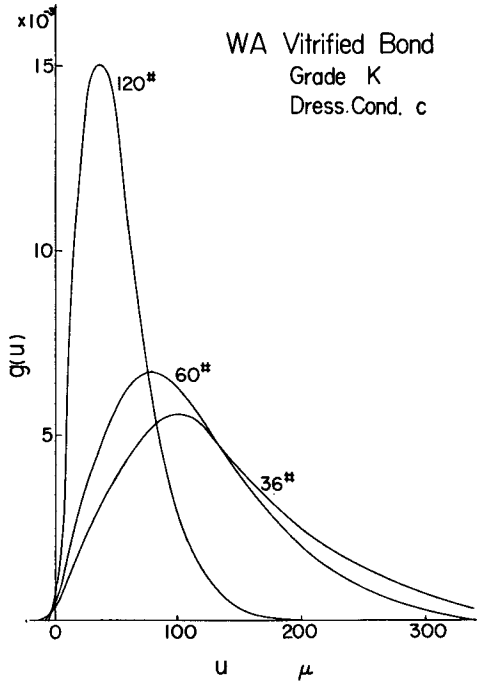

Fig. 11. Analytical cutting edge distribution

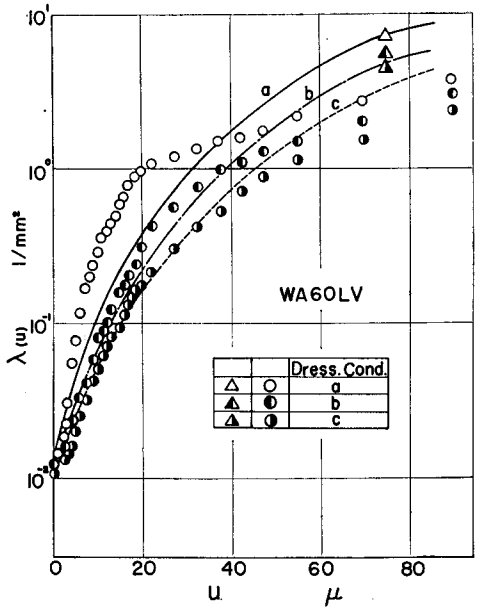

Fig. 12. Three dimensional density of cutting edges for Vitrified wheel

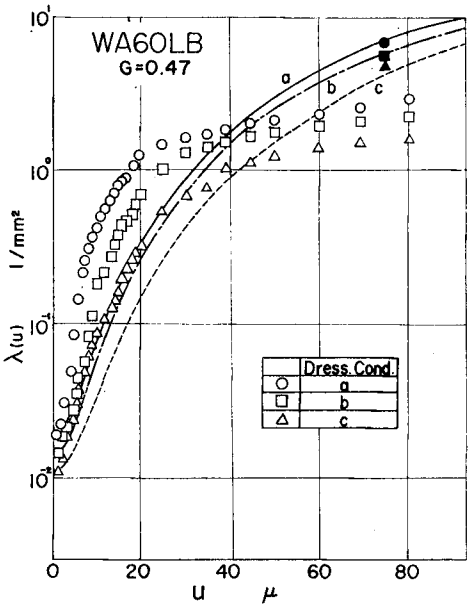

Fig. 13. Three dimensional density of cutting edges for Resinoid wheel

Figure 12 and Figure 13 show the three-dimensional density of cutting edges for the grinding wheels WA60LV and WA60LB dressed under three different conditions *a*, *b* and *c* respectively.

In these figures, plots show the density counted immediately, the smooth curve calculated by Equation (9) and three black points at the depth $u=75\ \mu$ that are evaluated from the copies of the surface of the wheel obtained by direct contact method as shown in Figures 14 to 16. Figure 17 and Figure 18 show the variation of three-dimensional distribution $\lambda(u)$ of cutting edges with the bond ratio for the vitrified and the resinoid bond wheel for dressing condition (b) respectively. Figure 19 shows the variation of $\lambda(u)$ with grain size for vitrified bond wheel. In these figures the depth u from the surface of the wheel is a parameter.

From Figures 12 to 19 we can easily see the relation between the three-dimensional density $\lambda(u)$ of cutting edges and grain size, bond ratio and dressing conditions.

3. Static Spring Constant of Grain Mounting

The properties of the grinding wheel have been indicated by the grade measured by the scale of plastic deformation, but the properties of grinding wheel should be indicated by the value measured by the scale of elastic deformation from the point of view of chip formation physics.

Elastic properties of the grinding wheel have been investigated by many

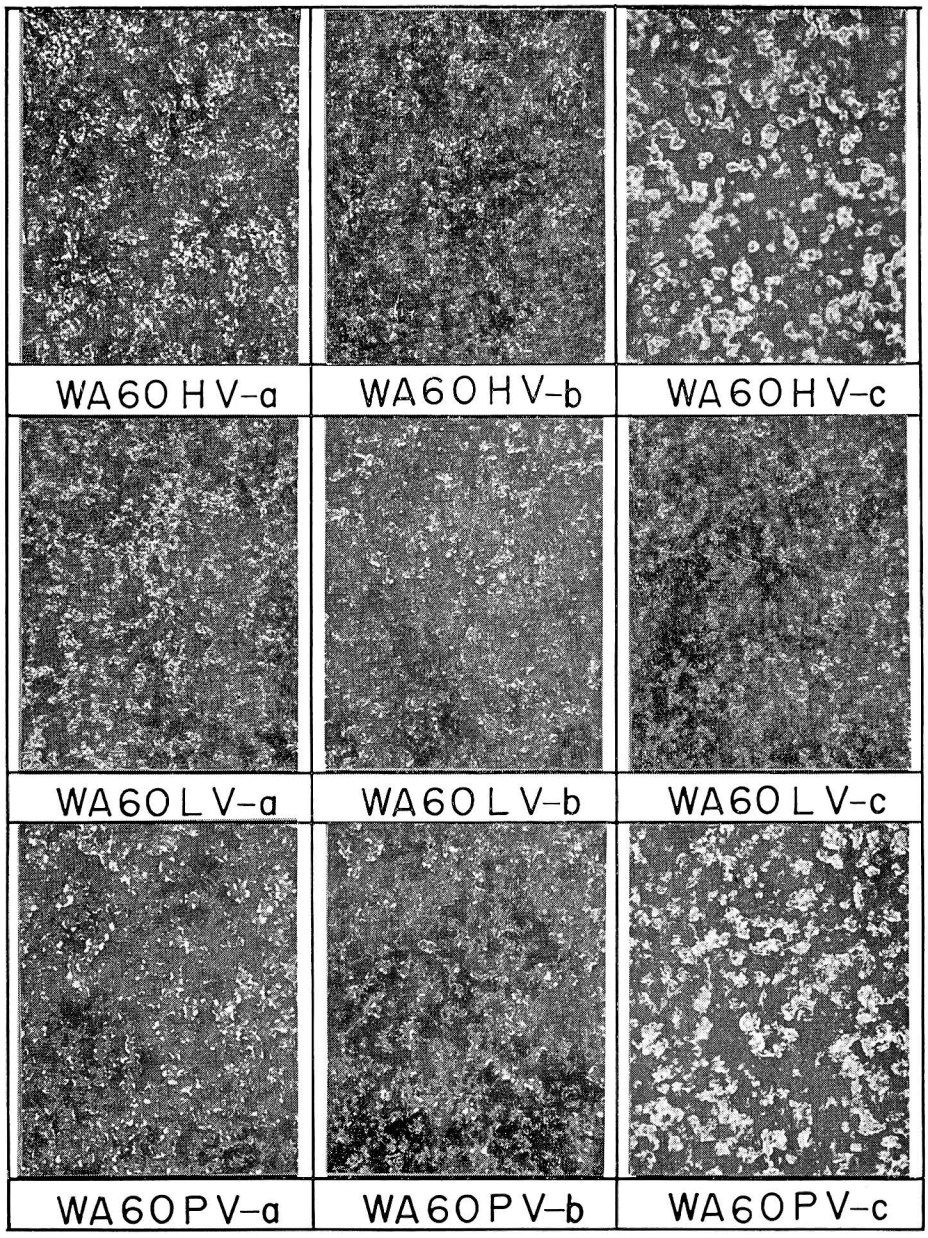

Fig. 14. Surface of Vitrified wheels by direct contact method

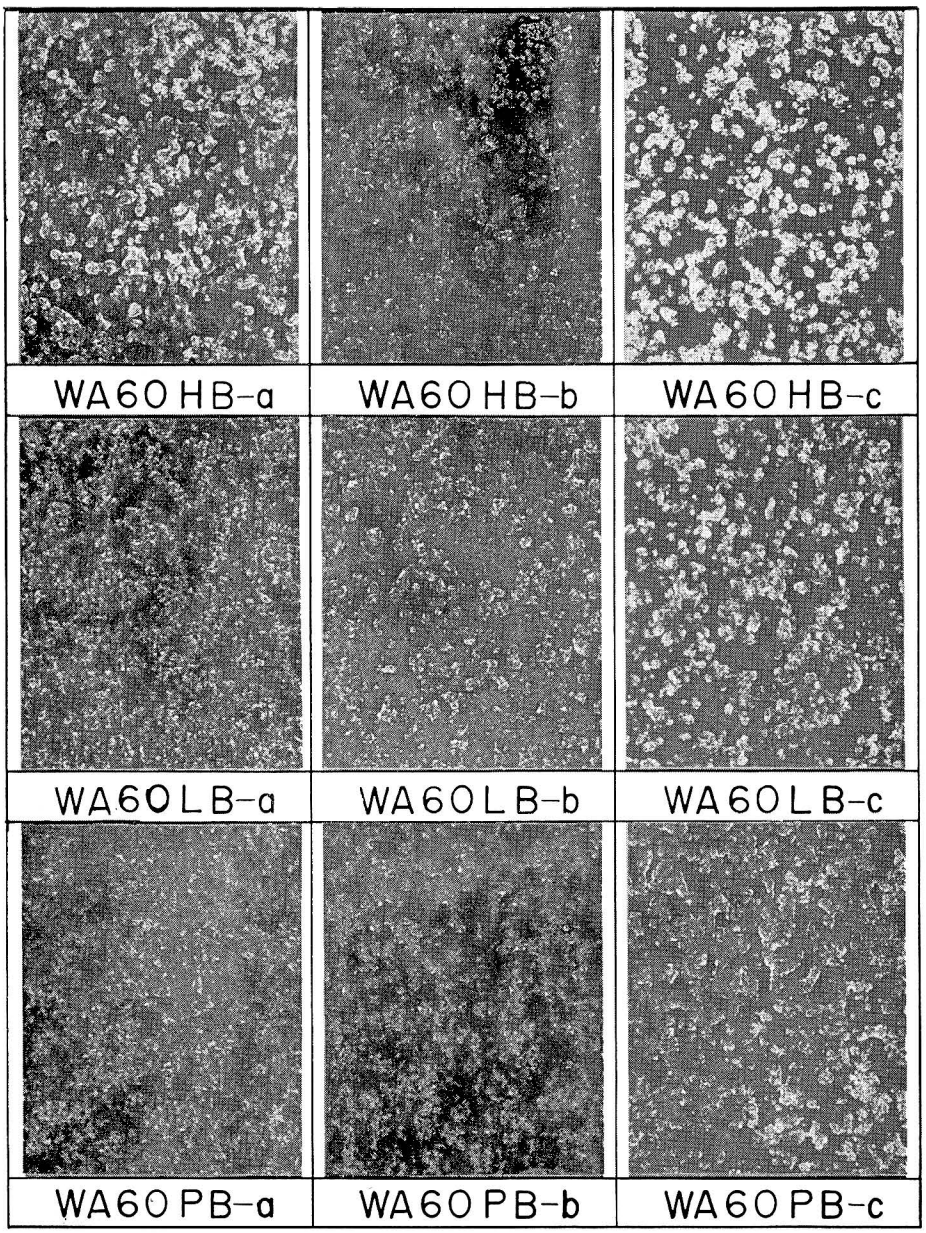

Fig. 15. Surface of Resinoid wheels by direct contact method

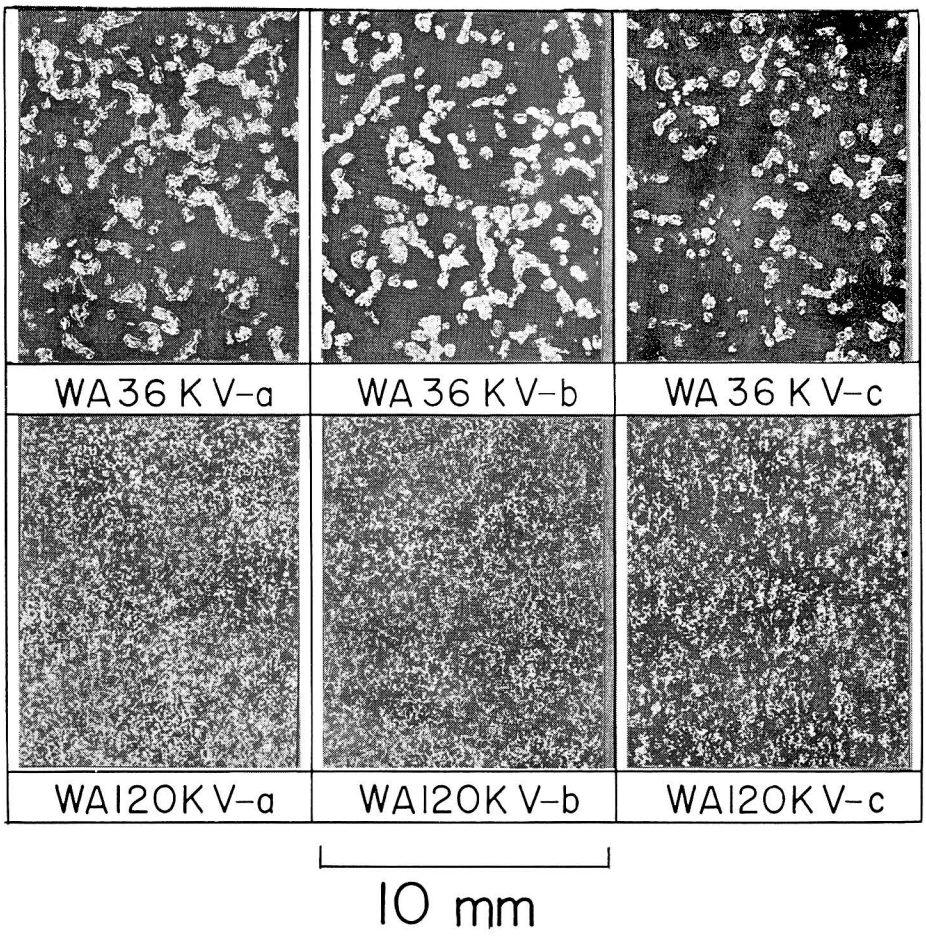

Fig. 16. Surface of Vitrified wheels by direct contact method for different grain size

researchers since Dr. R.S. Hahn discussed the effect of elastic displacement of cutting edges on the grinding process for the first time. But almost all of them are macroscopic modulus of elasticity of the wheel composed of grains, bond and pores.

Seeing that each grain in the interference zone supports the grinding load and displaces almost separately in practical grinding, the spring constant of grain mounting has a stronger physical meaning on the cutting process of abrasive grain than the modulus of elasticity of the wheel. From this point of view the spring constant of grain mounting will be measured based on the three-dimensional distribution of cutting edges determined in the previous section and the relations between the spring constant and grain size, material of bond, bond ratio and dressing conditions by which the properties of grinding wheel may be affected

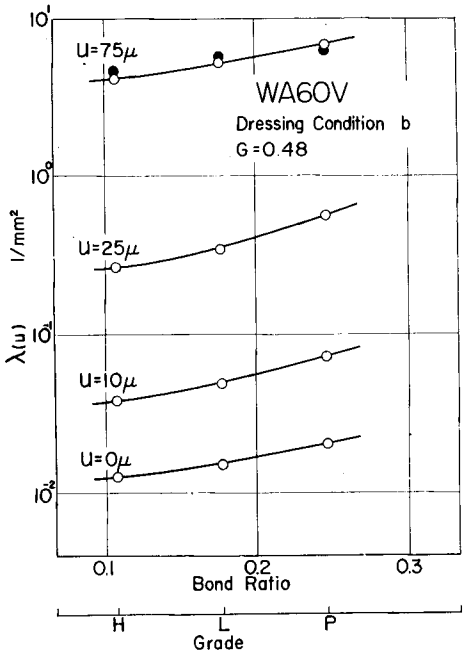

Fig. 17. Variations of density with grade for Vitrified wheel

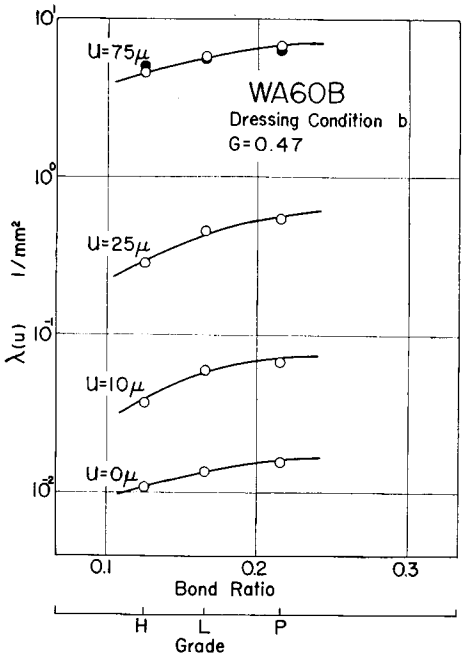

Fig. 18. Variations of density with grade for Resinoid wheel

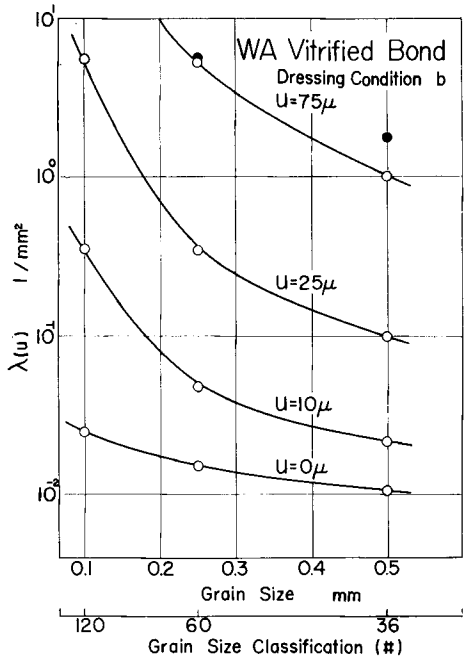

Fig. 19. Variations of density with grain size for Vitrified wheel

will be discussed. The relation between the grade and the spring constant of grain mounting will also be discussed.

3.1 Experimental Method and Apparatus

As shown in Figure 20, the push bar which has a constant cross section (12 mm × 12 mm) is pressed on the surface of the wheel and the force P acting on the push bar and the displacement u of the push bar into the wheel are measured at the same time.

The experimental apparatus is shown in Figure 21. Tool dynamometer (1) is fixed on the table of a cylindrical grinder and the push bar (2) made of quenched Cr-Mo steel is mounted on the dynamometer. On the push bar the

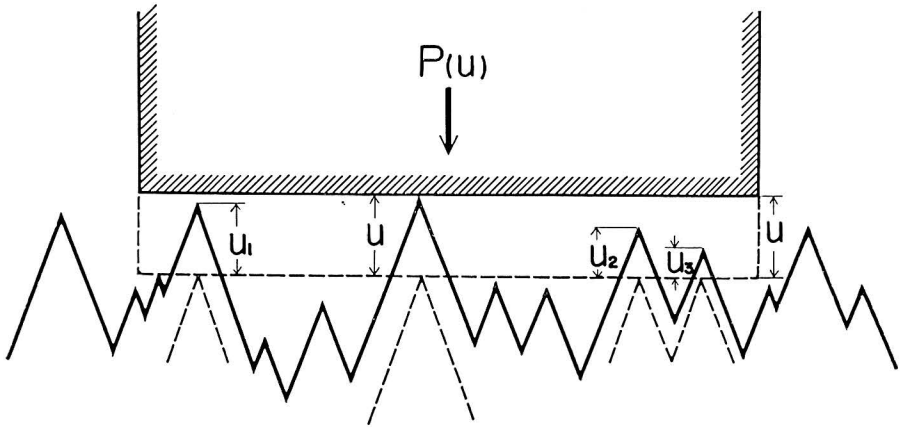

Fig. 20. Push bar acting on a wheel

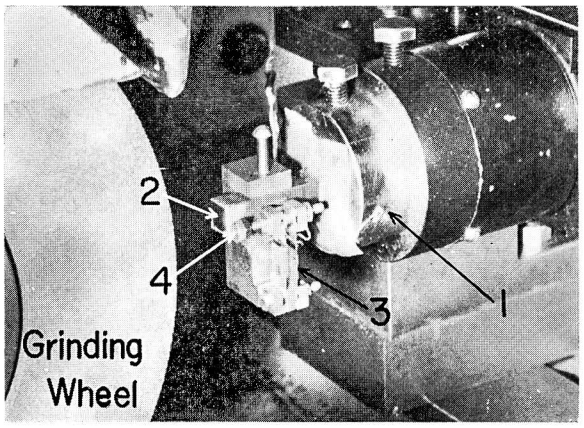

Fig. 21. Experimental apparatus

probe of a highly sensitive contacting displacement gauge (4) is set up approximately 2 μ closer to the wheel than the front of the push bar. The curvature of the front face of the push bar is made the same as that of wheel and the hardness of the front of the push bar is about 60 R_c and, therefore, the indentation of cutting edges into the push bar will be negligible.

Now the apparatus is fed onto the surface of the wheel at a constant speed by automatic plunge, first the displacement gauge hits the wheel and then the push bar hits. The force P and the displacement u are recorded at the same time and the load displacement curve (P-u curve) is obtained. The kinds and structure of the wheels used in this experiment are shown in Table 1 and the dressing conditions in Table 2.

3.2 Evaluating Method of the Spring Constant of Grain Mounting

As mentioned in the previous section, the density $\lambda(u)$ of the cutting edges becomes more dense with the increase of the depth u from the surface of wheel and, therefore, the spring constant of mounting of grains also becomes stiffer with the depth u.

Now assume that cutting edges are mounted resiliently by non-linear springs, the initial spring constants being a function of the depth u from the surface. In other words, the spring constant of grain mounting of cutting edges just on the surface is $k(0)$ under no displacement and becomes $k(u)$ when the cutting edges displace to the depth u. Furthermore the spring constant of cutting edges at the depth u is equal to $k(u)$.

As shown in Figure 20, when the push bar of cross section area S is indented into the surface up to the depth u, all the cutting edges between o and u under the push bar will displace up to the position of the depth u. Then the spring constant of all cutting edges at the depth u are equal to $k(u)$ on the above mentioned assumption, and, therefore, the increment of force dP necessary to displace the push bar further by an infinitesimal depth du is given by the equation,

$$dP = s \cdot k(u) \cdot \lambda(u) \cdot du \tag{10}$$

Then

$$k(u) = \frac{1}{\lambda(u)} \frac{d}{du}\left(\frac{P}{s}\right) = \frac{1}{\lambda(u)} \frac{dp}{du} \tag{11}$$

where $p=P/s$

The three-dimensional density of cutting edges $\lambda(u)$ can be calculated by Equation (9). Therefore, if we can experimentally evaluate the slope dp/du of the P-u curve, the spring constant of grain mounting $k(u)$ will be evaluated by Equation (11).

3.3 Theoretical Analysis of Spring Constant of Grain Mounting on the Surface $k(o)$

Grinding wheels are composed of three elements, abrasive grains, bond and pores. Assuming that abrasives are spheres of diameter d_0, that the shape of bond bridges by which abrasives are mounted is cylindrical as shown in Figure 22(a) and that abrasives are located at the tops of a tetrahedrons as shown in Figure 22(b), then the diameter of the bond bridges (d_b) and the distance between two abrasives (l) are given in the form

$$\left.\begin{aligned} l &= \sqrt[3]{\frac{\sqrt{2\pi}}{5V_G}}\, d_0 \\ d_b &= \sqrt{\frac{2V_B}{3\sqrt{2\pi}\left(1-\sqrt[3]{5V_G\sqrt{2\pi}}\right)}}\, l \end{aligned}\right\} \tag{12}$$

where V_G is grain volume ratio and V_B is bond volume ratio. Let us consider

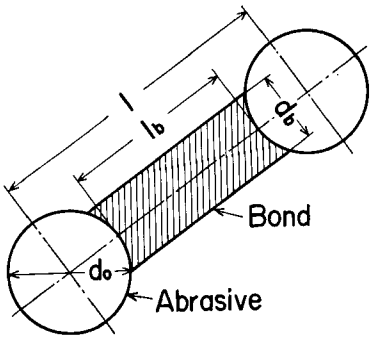

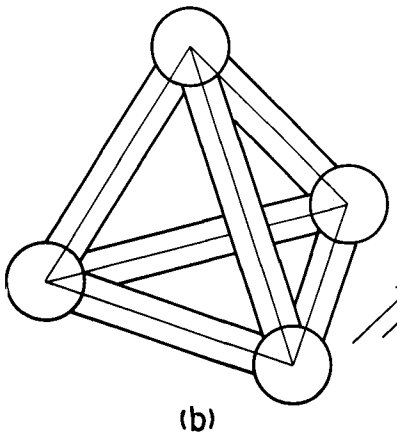

Fig. 22. Model of grain mounting

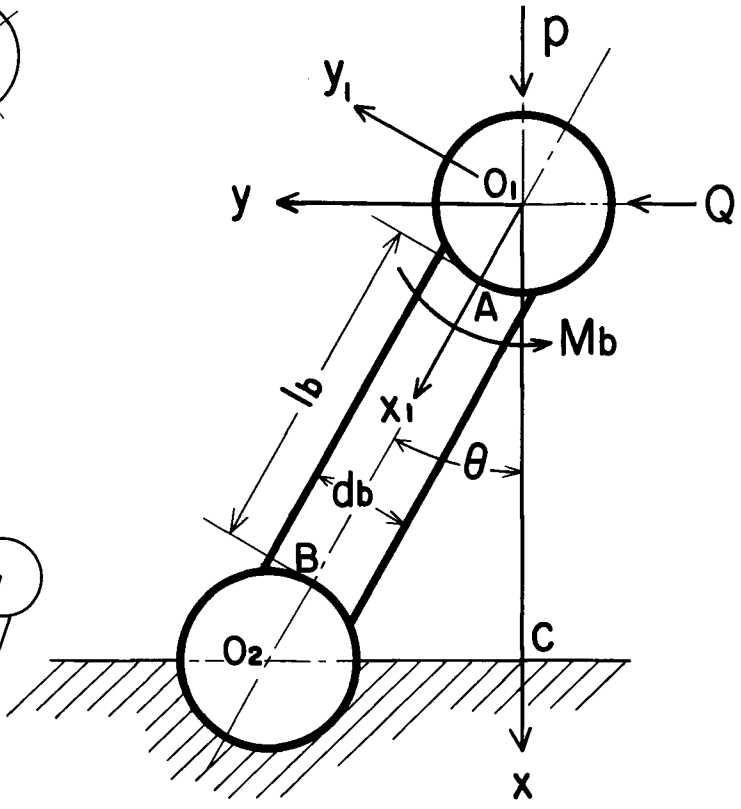

Fig. 23. Analysis of spring constant of grain mounting on surface

the displacement x of a grain in this construction for an applied force P in the direction from the center of the grain to that of the center of gravity of the construction.

In Figure 23, a grain 0_1 displaces in the x-direction by x. Denoting components in x_1 and y_1 directions of the external forces P and Q by Wx_1 and Wy_1 respectively, we find

$$\left.\begin{aligned} Wx_1 &= p\cos\theta + Q\sin\theta \\ Wy_1 &= p\sin\theta - Q\cos\theta \end{aligned}\right\} \tag{13}$$

where θ is an angle between x and x_1 axes and p is equal to $P/3$. An elastic energy U_a due to compression and bending and that U_b due to shear caused by the external forces are

$$\left.\begin{aligned} U_a &= \frac{32l_b^3 W_{y_1}^2}{3\pi d_b^4 E} + \frac{2l_b W_{x_1}^2}{\pi d_b^2 E} \\ U_b &= \frac{128 l_b W_{y_1}^2}{27\pi d_b^2}\cdot\frac{1+\nu}{E} \end{aligned}\right\} \tag{14}$$

where E is modulus of elasticity of bond material which is approximately equal to 6700 kg/mm^2 for Vitrified bond and 2680 kg/mm^2 for Resinoid bond. On the other hand, an elastic energy U_c due to the moment M_b is

$$U_c = \frac{8l_b^3 W_{y_1}^2}{\pi d_b^4 E} \tag{15}$$

Therefore, the total elastic energy U can be given in the form

$$U = (C_1 W_{y_1}^2 + C_2 W_{x_1}^2)/2 \tag{16}$$

where

$$\left.\begin{aligned} C_1 &= 2\left[\frac{56l_b^3}{3\pi d_b^4 E} + \frac{128(1+\nu)l_b}{27\pi d_b^2 E}\right] \\ C_2 &= 4l_b/\pi d_b^2 E \end{aligned}\right\} \tag{17}$$

The external force Q can be given, or the condition that the grain 0_1 does not displace in y direction, in the following equation;

$$Q = \frac{(C_1 - C_2)\sin\theta\cos\theta}{C_1\cos^2\theta + C_2\sin^2\theta}\cdot p \tag{18}$$

This displacement X of the grain 0_1 in the x direction is from Castigliano's theorem

$$X = \frac{\partial U}{\partial p} = C_1\sin\theta(p\sin\theta - Q\cos\theta) + C_2\cos\theta\ (p\cos\theta + Q\sin\theta) \tag{19}$$

Therefore, spring constant of grain mounting $k(0)$ on the surface can be given by the following equation;

$$k(0) = \frac{\pi d_b^2 E}{2l_b}\left[1 + 3/8\left\{\frac{7l_b^2}{d_b^2} + \frac{16(1+\nu)}{9}\right\}\right] \tag{20}$$

Figure 24 shows theoretical spring constant of grain mounting on the surface calculated by Equation (20). As can be seen in this figure, the spring constant $k(0)$ increases with increasing bond ratio and grain ratio.

3.4 Experimental Results

(1) An Example of the *P-u* Curve

Figure 25 shows an example of *P-u* curve recorded experimentally. Figure 26 shows an example of *P-u* curve both in loading and unloading recorded to investigate the hystersis phenomenon of the bond bridges. It can be seen from Figure 26 that these two curves fit and therefore that there seems to be no breakage of bond bridges and abrasives in the range of displacement of this experiment.

(2) The Slope of *P-u* Curve

The slope dp/du of the *P-u* curve at a certain point corresponds to the force necessary to displace the push bar a unit depth at that point and is, therefore, the fundamental value required to evaluate the spring constant of grain mounting. Figure 27 and Figure 28 show variation of the slope dP/du of the *P-u* curve with dressing conditions, Figure 29 and Figure 30 that with grade and Figure 31 that with grain size as a function of the depth u from the surface.

(3) The Density of Cutting Edges Near the Surface of the Wheel

The three-dimensional density $\lambda(u)$ of cutting edges was discussed in previous section and can be expressed as Equation (9).

Figure 32 to Figure 36 show the accumulative density $\lambda(u)$ of cutting edges near the surface of wheels. Figure 32 and Figure 33 show the effect of dressing conditions, Figure 34 and Figure 35 that of grade and Figure 36 that of grain size on the accumulative density as a function of the depth u from the surface respectively.

(4) The Spring Constant of Grain Mounting of Vitrified and Resinoid Bond Wheels

The spring constant of grain mounting can be calculated from Equation (11) by the increment dP/du shown in Figure 27 to Figure 31 and the density $\lambda(u)$ shown in Figure 32 to Figure 36. Figure 37 and Figure 38 show the effect of dressing conditions on the spring constant for vitrified and resinoid bond wheels respectively.

In these figures it can be seen that the spring constant $k(u)$ becomes larger with the depth from the surface and from finer dressing for both the vitrified and resinoid bonded wheels. Figure 39 and Figure 40 show the relation between the grade

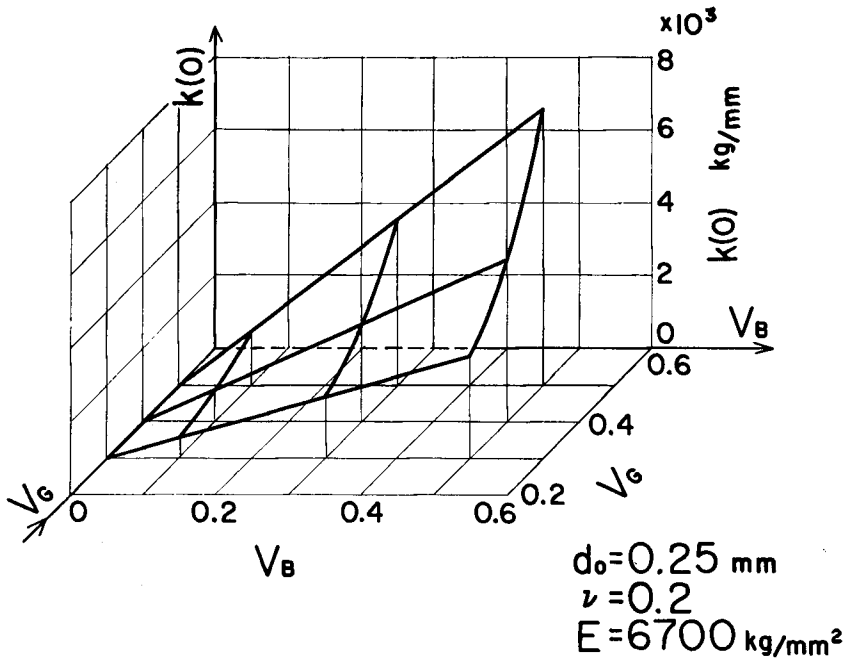

Fig. 24. Theoretical spring constant of grain mounting on surface

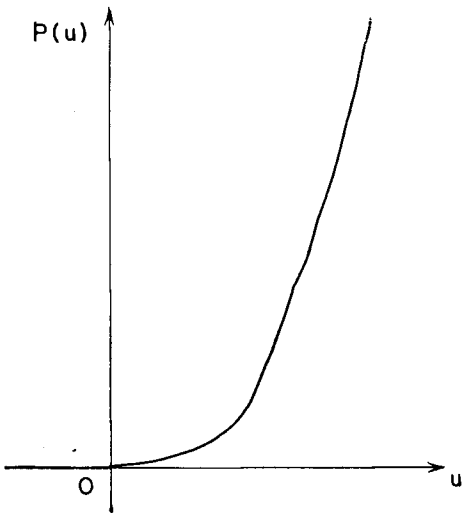

Fig. 25. Force-displacement curve of wheel

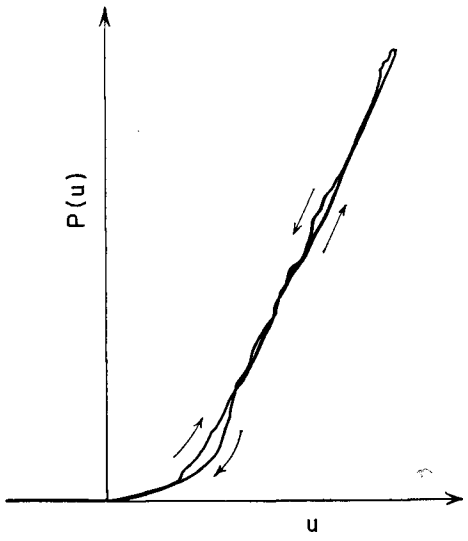

Fig. 26. Force-displacement curve showing hysteresis

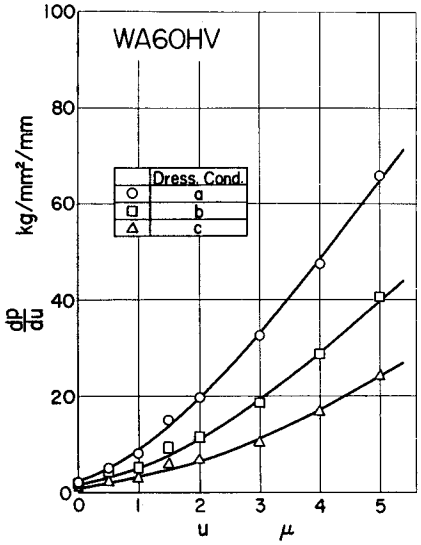

Fig. 27. Variations of slope of force-displacement curve with depth from the surface of wheel for dressing conditions (Vitrified wheel)

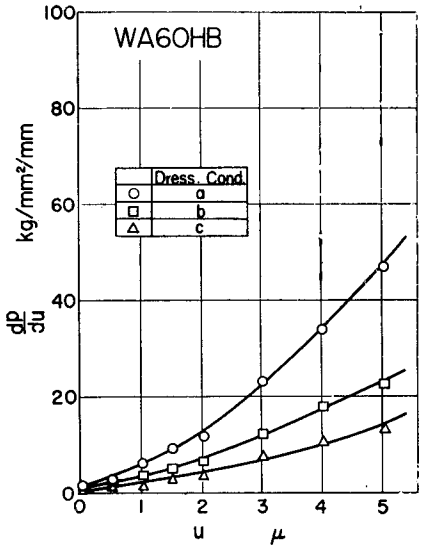

Fig. 28. Variations of slope of force-displacement curve with depth from the surface of wheel for dressing conditions (Resinoid wheel)

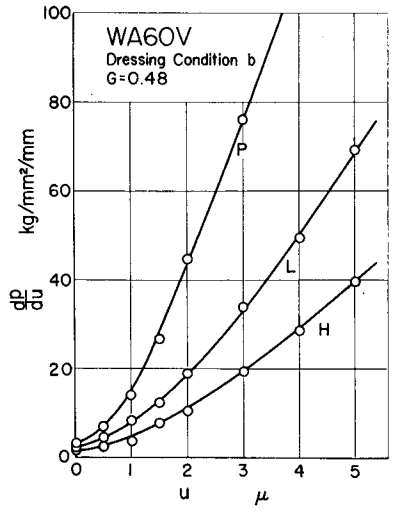

Fig. 29. Variations of slope of force-displacement curve with depth from the surface of wheel for grade (Vitrified wheel)

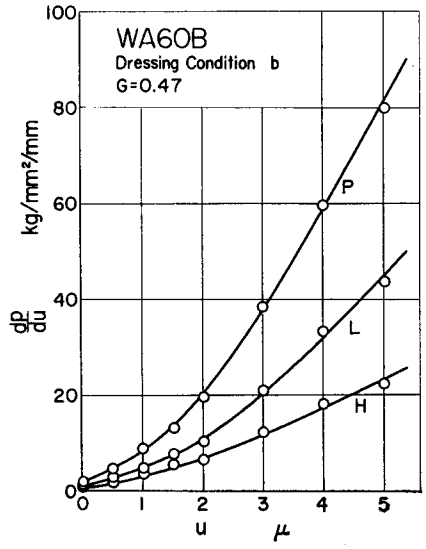

Fig. 30. Variations of slope of force-displacement curve with depth from the surface of wheel for grade (Resinoid wheel)

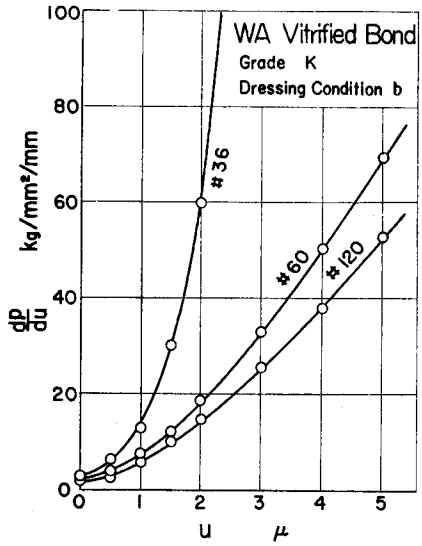

Fig. 31. Variations of slope of force-displacement curve with depth from the surface of wheel for grain size

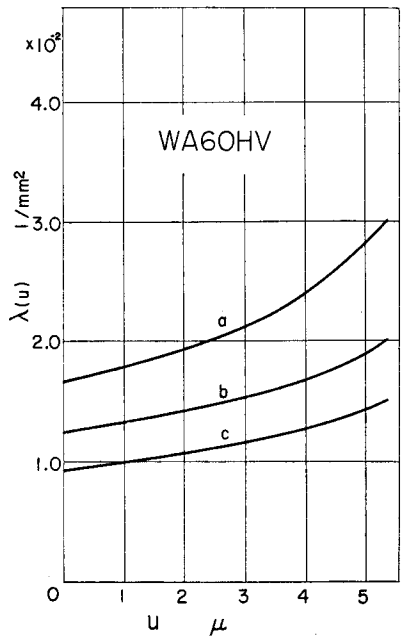

Fig. 32. Variations of cumulative density of cutting edge for dressing conditions (Vitrified wheel)

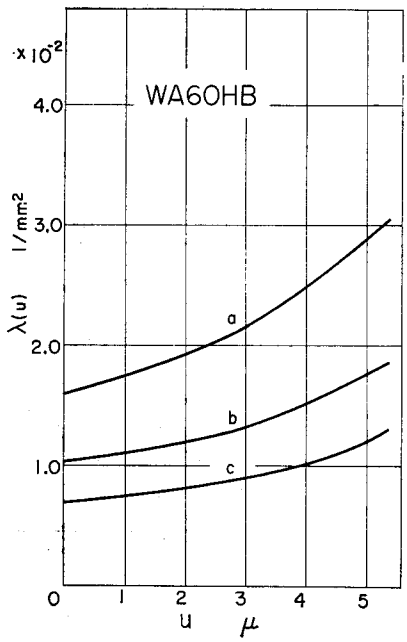

Fig. 33. Variations of cumulative density of cutting edge for dressing conditions (Vitrified wheel)

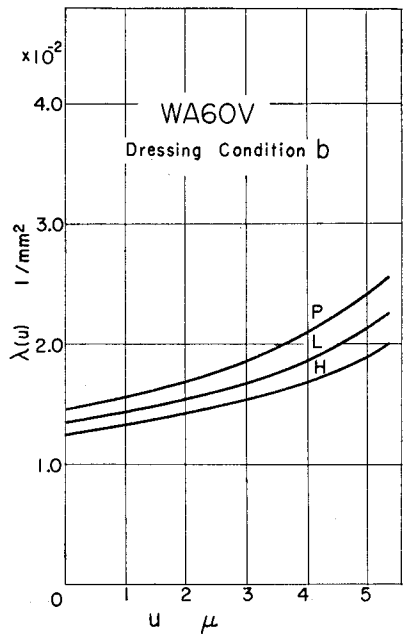

Fig. 34. Variations of cumulative density of cutting edge for grade (Vitrified wheel)

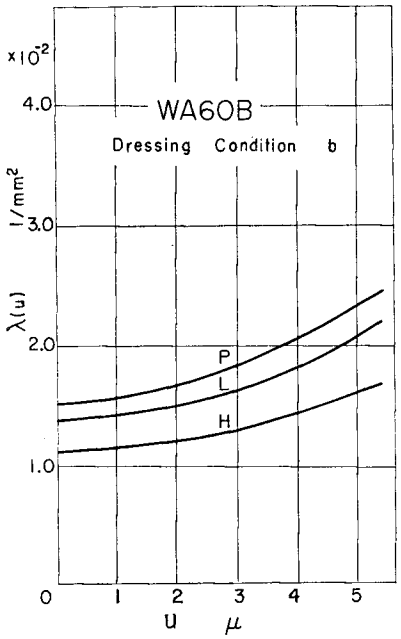

Fig. 35. Variations of cumulative density of cutting edge for grade (Resinoid wheel)

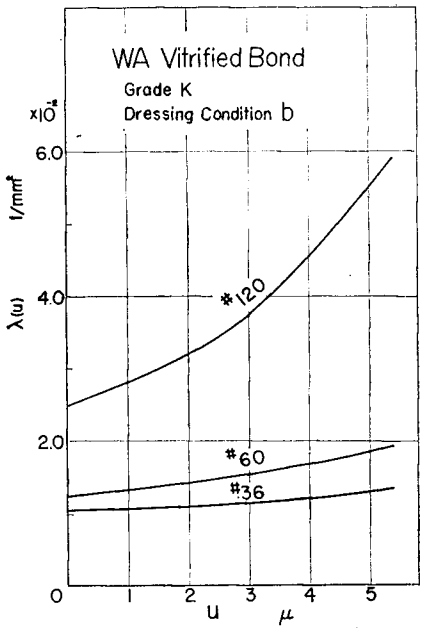

Fig. 36. Variations of cumulative density of cutting edge for grain size

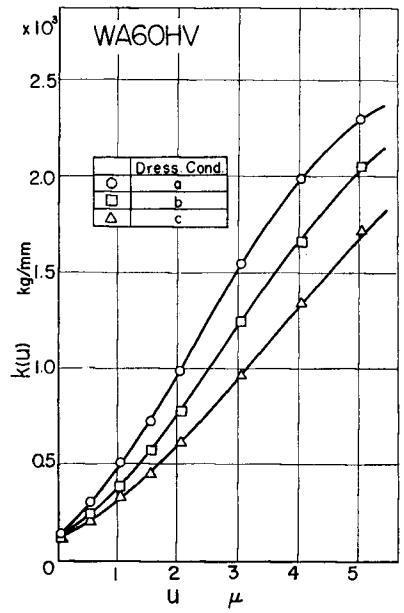

Fig. 37. Effects of dressing conditions on spring constant (Vitrified wheel)

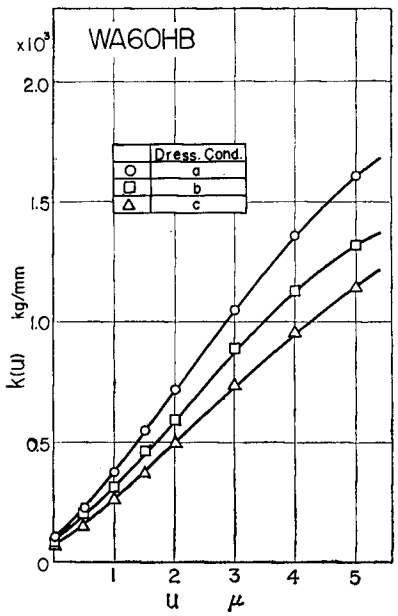

Fig. 38. Effects of dressing conditions on spring constant (Resinoid wheel)

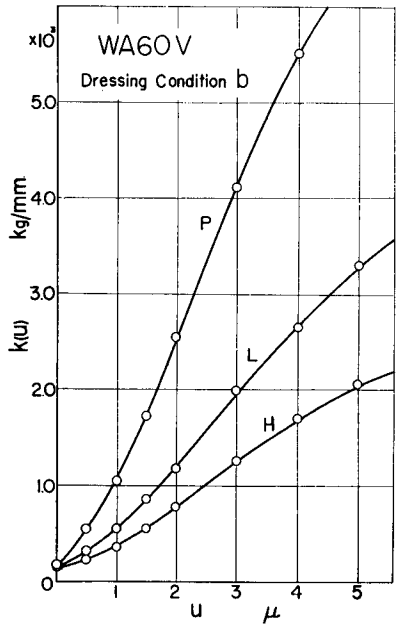

Fig. 39. Relations between grade and spring constant (Vitrified wheel)

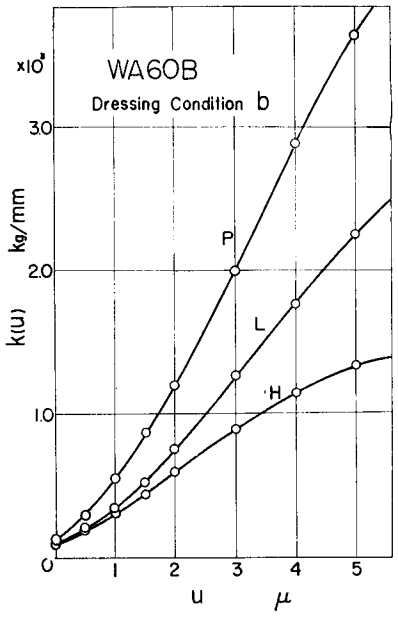

Fig. 40. Relations between grade and spring constant (Resinoid wheel)

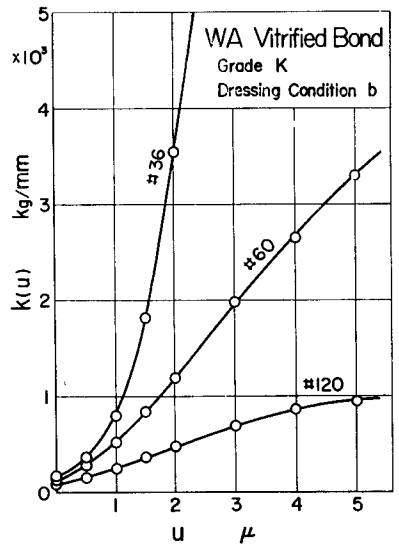

Fig. 41. Relations between grade and spring constant

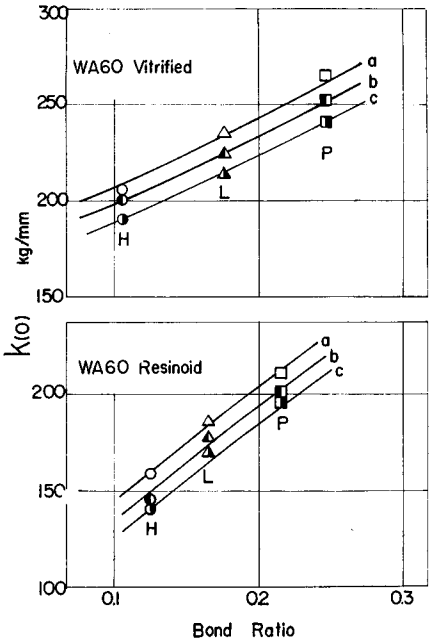

Fig. 42. Variations of spring constant on surface of wheel with bond ratio

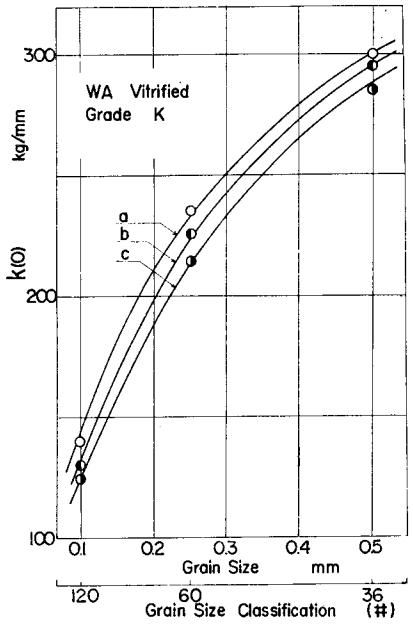

Fig. 43. Variations of spring constant on surface of wheel with grain size

and the spring constant under a fixed dressing condition for vitrified and resinoid bond wheels respectively. These figures show that the spring constant of grain mounting becomes larger with a higher value of the grade in the case of constant grain ratio. Figure 41 shows variations of the spring constant with grain size for a vitrified bond wheel dressed in a fixed condition. Figure 42 and Figure 43 show variations of the spring constant $k(0)$ on the surface with bond ratio for vitrified and resinoid bond wheels and with grain size respectively.

(5) The Spring Constant of PVA Wheel

PVA wheel, a typical elastic wheel, is composed of grain mounted on spongy vinylon and, therefore, has a very small spring constant. It is impossible to dress these wheels with a diamond form dresser, so in this experiment the wheel was dressed with a vitrified wheel, WA60LV.

In this case it was very hard to measure the distribution of cutting edges because there were many peaks of vinylon on the surface. Therefore, the properties of these wheels should be indicated by the slope of P-u curve for the spring constant of grain mounting. Figure 44 shows an example of P-u curve for PVA wheels.

It can be seen that the force P has a linear relation to the displacement u and therefore, the force dP/du necessary to displace the wheel by a unit depth is constant with the depth of the surface. Figure 45 shows variation of the force increment dP/du with percentage of hardner which is added in the process of manufacturing the wheel.

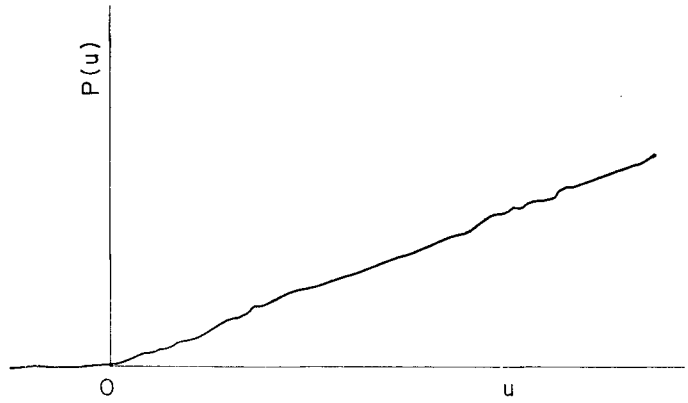

Fig. 44. Example of force-displacement curve for P.V.A. wheel

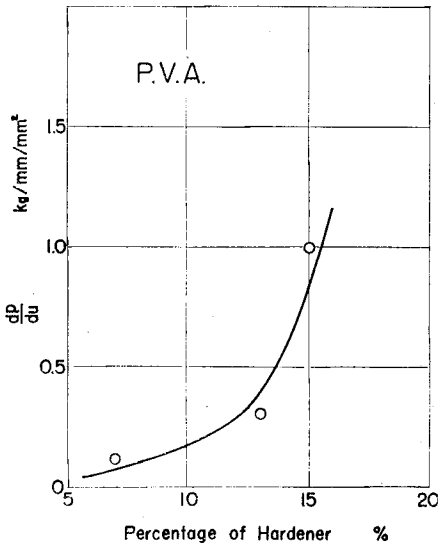

Fig. 45. Variations of slope of *P-u* curve with percentage of hardener

4. Conclusions

The elastic properties of a grinding wheel, which affect the grinding results such as grinding efficiency and surface integrity, should be represented by the spring constant of grain mounting from the view-point of chip formation physics, because each grain in the interference zone bears the grinding load and displaces almost separately in a practical grinding.

The spring constant of grain mounting is an important value to clarify the behavior of the cutting edges during grinding which affects the grinding process.

From this point of view, in this paper the three-dimensional distribution of

cutting edges, which is necessary for analyzing the spring constant and the simultaneously acting number of cutting edges, has been first analysed.

Then the spring constant of grain mounting has been measured and the relations between the spring constant and grain size, bond materials, bond ratio and dressing conditions have been discussed.

References

1) M. Okoshi and H. Watanabe: Study on Grade of Grinding Wheel, jour. JSPE, Vol. 18, No. 4, No. 6–7, No. 9, No. 11–12
2) R. Peklenik, R. Lane and M.C. Shaw: Comparison of Static and Dynamic Hardness of Grinding Wheels, Trans. ASME, Aug. (1964), 294
3) R.S. Hahn: The Effect of Wheel-Work Conformity in Precision Grinding, Trans. ASME, Vol. 77, No. 8 (1955)
4) H. Münich: Beitrag zur Sicherheit von umlaufenden Schleifhörpern, Diss. T.H., Hannover (1965)
5) H. Krug and G. Honica: Die elastische Verformung bei Schleifwerkzeugen, Werkstattstechnik 54 (1964), Heft 2, s53